საქართველოს მეცნიერებათა ეროვნული აკადემიის მოამბე, ტ. 20(194), №2, 2026
BULLETIN OF THE NATIONAL ACADEMY OF SCIENCES OF GEORGIA, vol. 20(194), no. 2, 2026

Physics

Phases and Currents in 2D Tight-Binding Model on a Strip Geometry

Merab Eliashvili[*,**], **George Tsitsishvili**[*,**]

[*] *Department of Physics, Tbilisi State University, Tbilisi, Georgia*
[**] *Department of Theoretical Physics, A. Razmadze Mathematical Institute, Tbilisi, Georgia*

(Presented by Academy Member George Japaridze)

Abstract. The tight-binding model on a lattice strip with hopping anisotropies is considered. The system may exhibit three different phases – bulk, edge and mixed. The edge phase may itself occur in three different modifications. We comment on the possible current configurations corresponding to each of these edge-state cases. *© 2026 Bull. Natl. Acad. Sci. Georg.*

Keywords: tight-binding model, edge states, currents

Introduction

The main imprint of a topological order in two-dimensional electron systems is the occurrence of edge state (Bernrvig & Hughes, 2013). The physics of edge states has become the subject of intense studies due to the progress in the fabrication of low-dimensional electron structures. The common approach for studying such systems is the tight-binding models (Altland & Simons, 2006; Asboth et al., 2016) of various geometric configurations, both with and without boundaries. In the present paper, we consider a tight-binding model of free electrons living on a two-dimensional square lattice ribbon. Electron delocalization is characterized by four nearest neighbor hopping parameters. The simplified version of this model has been studied in (Eliashvili et al., 2014), where the eigenvalue equation is reduced to a three-term recurrence relation by turning off one of the four hopping parameters. In that case the occurrence of edge and bulk state has been described in the exact analytic way in terms of the Chebyshev polynomials. In the present work, we maintain all four parameters leading to a five-term recurrence relation and show that three different phases may develop: 1) simultaneous occurrence of two bulk states with two different oscillation lengths; 2) simultaneous occurrence of two edge states with two different penetration depths and 3) simultaneous occurrence of one bulk and one edge state.

The Model

We consider the tight-binding model on a strip shown in Fig. 1. The corresponding tight-binding Hamiltonian appears as

$$\begin{aligned} H = {} & t_{\uparrow} \sum_{m} \sum_{n=1}^{N} [c_{\circ}^{\dagger}(n,m) c_{\bullet}(n,m) + h.c.] + \\ & + t_{\downarrow} \sum_{m} \sum_{n=1}^{N} [c_{\circ}^{\dagger}(n,m-1) c_{\bullet}(n,m) + h.c.] + \\ & + t \sum_{m} \sum_{n=2}^{N} [c_{\circ}^{\dagger}(n-1,m-1) c_{\bullet}(n,m) + h.c.] + \\ & + t' \sum_{m} \sum_{n=1}^{N-1} [c_{\circ}^{\dagger}(n+1,m) c_{\bullet}(n,m) + h.c.], \end{aligned} \tag{1}$$

where the symbols "•" and "∘" label the Bravais sublattices. Fourier transform of (1) gives

$$H = \oint (C_{\bullet}^{\dagger}, C_{\circ}^{\dagger}) \begin{pmatrix} 0 & T^{\dagger} \\ T & 0 \end{pmatrix} \begin{pmatrix} C_{\bullet} \\ C_{\circ} \end{pmatrix} dk \tag{2}$$

$$T = t_{\uparrow} + t_{\downarrow} e^{+ik} + t e^{+ik} \beta^{\dagger} + t' \beta \tag{3}$$

$$\beta = \begin{pmatrix} 0 & 0 & 0 & \cdots & 0 & 0 \\ 1 & 0 & 0 & \cdots & 0 & 0 \\ 0 & 1 & 0 & \cdots & 0 & 0 \\ \vdots & \vdots & \vdots & \ddots & \vdots & \vdots \\ 0 & 0 & 0 & \cdots & 0 & 0 \\ 0 & 0 & 0 & \cdots & 1 & 0 \end{pmatrix} \tag{4}$$

$$C_{\mu}(k) = \{c_{\mu 1}(k), c_{\mu 2}(k), \ldots, c_{\mu N}(k)\}^{T}, \tag{5}$$

where $\mu = \bullet, \circ$. Let $\psi_{\bullet i}(k)$ and $\psi_{\circ i}(k)$ with $i = 1,2,\ldots,N$ be the solutions to the system

$$\begin{cases} T(k)\psi_{\bullet i}(k) = \mathcal{E}_{\nu}(k)\psi_{\circ i}(k) \\ T^{\dagger}(k)\psi_{\circ i}(k) = \mathcal{E}_{\nu}(k)\psi_{\bullet i}(k) \end{cases} \tag{6}$$

with $\mathcal{E}_i(k) \geq 0$. Then the positive and negative energy eigenstates of (2) are given by

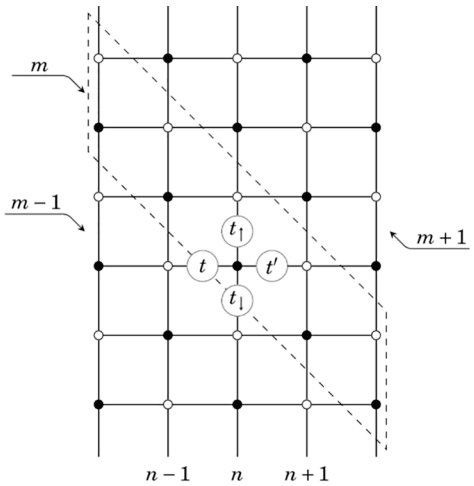

Fig. 1. Lattice strip with four-fold hopping anisotropy.

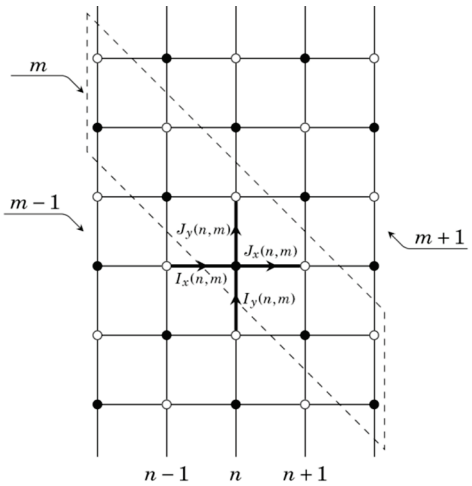

Fig. 2. Incoming and outgoing currents.

$$\begin{pmatrix} 0 & T^{\dagger} \\ T & 0 \end{pmatrix} \begin{pmatrix} \psi_{\bullet i} \\ \pm\psi_{\circ i} \end{pmatrix} = \pm\mathcal{E}_i(k) \begin{pmatrix} \psi_{\bullet i} \\ \pm\psi_{\circ i} \end{pmatrix}, \tag{7}$$

Expand the operators $c_{\mu n}(k)$ as

$$c_{\mu n}(k) = \sum_{i=1}^{N} \left[\psi_{\mu i}(k)\right]_n f_{\mu i}(k) \tag{8}$$

and introduce $\sqrt{2}f_{\pm i}(k) = f_{\bullet i}(k) \pm f_{\circ i}(k)$. Then the Hamiltonian (2) appears as

$$H = \int \sum_{i=1}^{N} \mathcal{E}_i(k) f_{+i}^{\dagger}(k) f_{+i}(k) dk - \int \sum_{i=1}^{N} \mathcal{E}_i(k) f_{-i}^{\dagger}(k) f_{-i}(k) dk, \tag{9}$$

so that $f_{\pm i}^{\dagger}(k)$ and $f_{\pm i}(k)$ are the creation and annihilation operators with energies $\pm\mathcal{E}_i(k)$.

Searching for the solutions as $[\psi_{\bullet i}]_n = e^{-(i/2)nk}[\xi_i]_n$ and $[\psi_{\circ i}]_n = e^{-(i/2)nk}[\zeta_i]_n$ we pass to

$$\begin{cases} \left(t_{\uparrow} e^{-(i/2)k} + t_{\downarrow} e^{+(i/2)k}\right)\xi_n + t\xi_{n+1} + t'\xi_{n-1} = \mathcal{E} e^{-(i/2)k}\zeta_n & \text{(10a)} \\ \left(t_{\uparrow} e^{+(i/2)k} + t_{\downarrow} e^{-(i/2)k}\right)\zeta_n + t\zeta_{n-1} + t'\zeta_{n+1} = \mathcal{E} e^{+(i/2)k}\xi_n & \text{(10b)} \end{cases}$$

Eliminating ζ_n from (10b) by means of (10a) we obtain

$$tt'\xi_{n+2} + \lambda^*\xi_{n+1} - \omega\xi_n + \lambda\xi_{n-1} + tt'\xi_{n-2} = 0 \tag{11a}$$

$$\lambda \equiv (t't_{\uparrow} + tt_{\downarrow})e^{+(i/2)k} + (t't_{\downarrow} + tt_{\uparrow})\, e^{-(i/2)k} \tag{11b}$$

$$\omega \equiv \mathcal{E}^2 - t_{\uparrow}^2 - t_{\downarrow}^2 - 2t_{\uparrow}t_{\downarrow}\cos k - t^2 - t'^2. \tag{11c}$$

We search for the solutions to (11a) in the form of $\xi_n = z^n$ and come to the equation

$$tt'z^4 + \lambda^* z^3 - \omega z^2 + \lambda z + tt' = 0. \tag{12}$$

Then the general solution to (11a) appears as

$$\xi_n = A_1 z_1^n + A_2 z_2^n + A_3 z_3^n + A_4 z_4^n, \tag{13}$$

where $z_{1,2,3,4}$ are the four complex roots of (12), and $A_{1,2,3,4}$ are the coefficients to be fixed by the boundary conditions (which we do not consider here). If any complex number z is the root of (12), then $1/z^*$ is the root as well. Therefore, we may have three different cases of how the four roots are distributed on a complex plane. These are: 1) all four roots are on the unit circle; in that case the wave function ξ_n oscillates with respect to n implying the bulk (*B*) state; 2) none of the roots are on the unit circle, i.e. two roots are within the unit circle and the rest two are outside thus signifying the genuine edge state (*E*) with two different length scales; 3) two roots are on the unit circle and the rest two are not, i.e. the mixture (*M*) of one edge and one bulk state. These cases can be written as

$$Bulk\ (B) \quad \left\{e^{+i(\alpha+\alpha_1)}, e^{-i(\alpha-\alpha_2)}, e^{+i(\alpha-\alpha_1)}, e^{-i(\alpha+\alpha_2)}\right\} \tag{14a}$$

$$Edge\ (E) \quad \{r_1 e^{+i\alpha}, r_2 e^{+i\alpha}, (1/r_1)e^{+i\alpha}, (1/r_2)e^{-i\alpha}\} \tag{14b}$$

$$Mixed\ (M) \quad \left\{r_1 e^{+i\alpha}, e^{-i(\alpha-\alpha_2)}, (1/r_1)e^{+i\alpha}, e^{-i(\alpha+\alpha_2)}\right\}, \tag{14c}$$

where $r_{1,2} < 1$, and $\alpha_{1,2}$ are the arguments on the complex plane.

In the first case we have two bulk states set by $\alpha_1$and α_2. In the second case we observe two edge states with the characteristic length scales set by r_1 and r_2. In the third case we have one edge state set by r_1 and one bulk state set by α_2.

Currents

We now discuss the possible current configurations in genuine edge states. For this purpose, we introduce the charge density operator $\rho_\bullet(n,m) = c_\bullet^\dagger(n,m)c_\bullet(n,m)$. Using the Heisenberg equation $i\partial_t\rho_\bullet(n,m) = [\rho_\bullet(n,m), H]$, we obtain the continuity equation

$$\partial_t\rho_\bullet(n,m) = I_x(n,m) + I_y(n,m) - J_x(n,m) - J_y(n,m), \tag{15}$$

where $I_{x,y}(n,m)$ and $J_{x,y}(n,m)$ represent the currents incoming to and outgoing from the site $r_\bullet(n,m)$ as shown in the Fig. 2. The corresponding expressions are given by

$$\begin{aligned} I_x(n,m) &= it\big[c_\circ^\dagger(n-1,m-1)c_\bullet(n,m) - c_\bullet^\dagger(n,m)c_\circ(n-1,m-1)\big] \\ I_y(n,m) &= it_\downarrow\big[c_\circ^\dagger(n,m-1)c_\bullet(n,m) - c_\bullet^\dagger(n,m)c_\circ(n,m-1)\big] \\ J_x(n,m) &= it'\big[c_\bullet^\dagger(n,m)c_\circ(n+1,m) - c_\circ^\dagger(n+1,m)c_\bullet(n,m)\big] \\ J_y(n,m) &= it_\uparrow\big[c_\bullet^\dagger(n,m)c_\circ(n,m) - c_\circ^\dagger(n,m)c_\bullet(n,m)\big]. \end{aligned} \tag{16}$$

Calculating the averages $\langle\{\cdots\}\rangle \equiv \langle 0|f_{\pm i}(k)\{\cdots\}f_{\pm i}^\dagger(k)|0\rangle$ one finds

$$\begin{aligned} 2\pi\mathcal{E}\langle I_x(n,m)\rangle &= \pm tIm\big[\big(t_\uparrow e^{-(i/2)k} + t_\downarrow e^{+(i/2)k}\big)\xi_n^*\xi_{n-1} + t'\xi_n^*\xi_{n-2}\big] \\ 2\pi\mathcal{E}\langle I_y(n,m)\rangle &= \pm t_\downarrow Im\big[t_\uparrow e^{-ik}\xi_n^*\xi_n + t'e^{-(i/2)k}\xi_n^*\xi_{n-1} + te^{-(i/2)k}\xi_n^*\xi_{n+1}\big] \\ 2\pi\mathcal{E}\langle J_x(n,m)\rangle &= \mp t'Im\big[\big(t_\uparrow e^{-(i/2)k} + t_\downarrow e^{+(i/2)k}\big)\xi_n^*\xi_{n+1} + t\xi_n^*\xi_{n+2}\big] \\ 2\pi\mathcal{E}\langle J_y(n,m)\rangle &= \pm t_\uparrow Im\big[t_\downarrow e^{+ik}\xi_n^*\xi_n + t'e^{+(i/2)k}\xi_n^*\xi_{n-1} + te^{+(i/2)k}\xi_n^*\xi_{n+1}\big], \end{aligned} \tag{17}$$

which lead to $\langle I_x(1,m)\rangle = \langle J_x(0,m)\rangle = \langle J_x(N,m)\rangle = \langle I_x(N+1,m)\rangle = 0$, thus implying no charge leak across the boundaries.

We comment on the question which of the three phases Eq. (16) occurs depending on the values of the hopping parameters. Comprehensive analysis of this topic is too complicated for general settings, and therefore we limit ourselves to the case of $t_\uparrow = t_\downarrow$. Let us introduce the dimensionless quantities:

$$u \equiv \frac{t_\uparrow\cos(k/2)}{\sqrt{tt'}}, \qquad \epsilon \equiv \frac{\mathcal{E}}{2\sqrt{tt'}}, \qquad \sinh\vartheta \equiv \frac{t-t'}{2\sqrt{tt'}} \tag{18}$$

and rewrite the quartic equation (12) as

$$\left(\frac{1}{2}\left[z + \frac{1}{z}\right] + u\cosh\vartheta\right)^2 + (1-u)^2\sinh^2\vartheta - \epsilon^2 = 0. \tag{19}$$

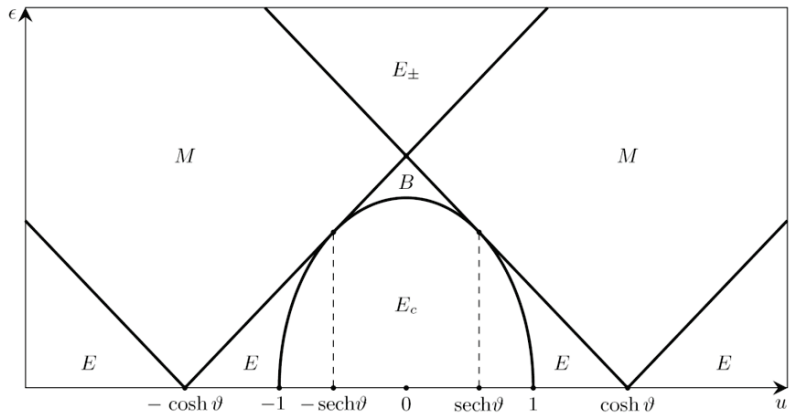

Fig. 3. Phases of possible one-particle states.

The four roots $z_{1,2,3,4}$ of (19) appear as the roots of the following two square equations

$$\frac{1}{2}\left(z+\frac{1}{z}\right) = -u\cosh\vartheta + \sqrt{\epsilon^2-(1-u)^2\sinh^2\vartheta} \tag{20a}$$

$$\frac{1}{2}\left(z+\frac{1}{z}\right) = -u\cosh\vartheta - \sqrt{\epsilon^2-(1-u)^2\sinh^2\vartheta}\,. \tag{20b}$$

For $\epsilon^2-(1-u)^2\sinh^2\vartheta<0$ the right-hand sides of (20) are complex, meaning that none of the four roots are on a unit circle (otherwise the left-hand sides are real). Therefore this phase implies the occurrence of genuine edge state (14b). We label this phase by E_c with E denoting "edge" and the subscript "c" indicating that the roots are complex.

For $\epsilon^2-(1-u)^2\sinh^2\vartheta>0$ the right-hand sides of (20) are real, hence $z+z^{-1}$ is real as well. If $z+z^{-1}<-2$ then z is real negative. For $-2<z+z^{-1}<2$ we find $z=e^{i\alpha}$, and for $z+z^{-1}>2$ the value of z is real positive. Detailed analysis of these options can be found in (Eliashvili & Tsitsishvili, 2025), while here we only itemize and comment on the outcomes of (20), which are collected in the Table below.

Table. List of possible one-particle states for $\epsilon^2-(1-u)^2\sinh^2\vartheta>0$

№	Label	Restrictions on u and ϵ^2	
1	E	$u>\mathrm{sech}\vartheta$	$(1-u^2)\sinh^2\vartheta<\epsilon^2<(u-\cosh\vartheta)^2$
2	M	$u>0$	$(u-\cosh\vartheta)^2<\epsilon^2<(u+\cosh\vartheta)^2$
3	B	$\lvert u\rvert<\mathrm{sech}\vartheta$	$(1-u^2)\sinh^2\vartheta<E^2<(\lvert u\rvert-\cosh\vartheta)^2$
4	$E_\pm$	$-\infty<u<+\infty$	$(\lvert u\rvert+\cosh\vartheta)^2<\epsilon^2$
5	M	$u<0$	$(u+\cosh\vartheta)^2<\epsilon^2<(u-\cosh\vartheta)^2$
6	E	$u<-\mathrm{sech}\vartheta$	$(1-u^2)\sinh^2\vartheta<\epsilon^2<(u+\cosh\vartheta)^2$

In the case №1 the four roots are all real negative numbers so the factors of $(-1)^n$ arising from z^n in (13) become irrelevant since can be factorized out as an overall phase. Therefore the case №1 is equivalent to the one №6 where all roots are real positive. These phases correspond to (14b) implying two edge states. We have denoted this phase as E.

In the case №2 two roots are phases ($e^{\pm i\alpha}$) and the rest two are real negative. Provided the two roots are phases, the negativity/positivity of the rest two roots does not make any sense. Therefore this is equivalent to case №5 (two roots are phases and the rest two are real positive). We denote these phases as M implying the mixture of edge and bulk states (14c).

In case №3, all roots are phases meaning the genuine bulk state (14a). We denote it by B.

In case №4, two roots are real positive while the rest two are real negative implying the case of two edge states (14b) which however differ from E since the factor of $(-1)^n$, occurring only in one pair of roots, cannot be factorized out. In order to distinguish this state from E, we denote it by $E_\pm$.

Collecting all the described cases, we construct the phase diagram shown in Fig. 3, where the areas corresponding to different phases are delimited by bold lines.

As pointed out, genuine edge states may occur in three different versions E, $E_\pm$ and E_c. The significant difference between E_c and the other two is that the solutions ξ_n are real for E and $E_\pm$, while they are complex for E_c. We then find that the currents across the strip all vanish $\langle I_x(n,m)\rangle=\langle J_x(n,m)\rangle=0$ for E and $E_\pm$, so the only nonvanishing currents are the ones along the strip

$$\langle I_y(n,m)\rangle = \langle J_y(n,m)\rangle = \frac{\mp t_\uparrow}{2\pi\mathcal{E}}\left[t_\uparrow \xi_n^2 \sin k + \xi_n(t\xi_{n+1} + t'\xi_{n-1})\sin(k/2)\right]. \quad (21)$$

In contrast, for E_c the currents across the strip are no longer zero and we may observe the current circulations around the elementary cells. Further study of this topic requires numerical calculations, which we consider as a separate project.

ფიზიკა

ფაზური მდგომარეობები და დენები მჭიდრო ბმის 2D მოდელში ზოლოვანი გეომეტრიით

მ. ელიაშვილი[*,**], გ. ციციშვილი[*,**]

[*] *ივანე ჯავახიშვილის სახ. თბილისის სახელმწიფო უნივერსიტეტი, ფიზიკის დეპარტამენტი, საქართველო*
[**] *ანდრია რაზმაძის სახელობის მათემატიკის ინსტიტუტი, თეორიული ფიზიკის განყოფილება, თბილისი, საქართველო*

(წარმოდგენილია აკადემიის წევრის გ. ჯაფარიძის მიერ)

ნაშრომში წარმოდგენილია მჭიდრო ბმის მოდელი ზოლოვანი გეომეტრიით. სისტემაში შეიძლება ჩამოყალიბდეს სამი სხვადასხვა მდგომარეობა – ოსცილაციური, კიდურა და შერეული. კიდურა მდგომარეობას გააჩნია ერთმანეთისგან განსხვავებული სამი სხვადასხვა ფორმა. ნაშრომში განხილულია დენების შესაძლო კონფიგურაციები კიდურა მდგომარეობებში. ნაჩვენებია, რომ კიდურა მდგომარეობების სამი შესაძლო ფორმიდან ორში წარმოიქმნება ზოლოვანი გეომეტრიის მიმართ მხოლოდ გასწვრივი დენი, ხოლო მესამე ფორმისას გასწვრივ დენთან ერთად წარმოიქმნება განივი დენიც, რაც მესრის ელემენტარულ უჯრედში დენის არანულოვან ცირკულაციაზე მიუთითებს.

REFERENCES

Altland, A., Simons, B. (2006). Condensed matter field theory, Cambridge University Press. https://doi.org/10.1017/CBO9780511804236

Asboth, J.K., Oroszlany, L., Palyi, A. (2016). A short course on topological insulators, Springer. https://doi.org/10.1007/978-3-319-25607-8

Bernevig, B.A., Hughes, T.L. (2013). Topological insulators and topological superconductors, Princeton University Press. https://doi.org/10.1515/9781400846733

Eliashvili, M., Japaridze, G.I., Tsitsishvili, G., Tukhashvili, G. (2014). Edge states in 2D lattices with hopping anisotropy and Chebyshev polynomials, J. Phys. Soc. Jpn. 83, 044706 (1-9). http://dx.doi.org/10.7566/JPSJ.83.044706

Eliashvili, M., Tsitsishvili, G. (2025). Topological phases in 2D tight-binding model on a ribbon, Transactions of A. Razmadze Mathematical Institute, 179, 393-397.

Received February, 2026